

Computational modelling of thermal loads on a heat storage for battery electric buses over service life

Veronika Stahl^{1,*}, Werner Kraft¹, Franz Lanzerath²

**Veronika Stahl (corresponding author), veronika.stahl@dlr.de*

¹*German Aerospace Center (DLR), Institute of Vehicle Concepts, Pfaffenwaldring 38-40, 70569 Stuttgart, Germany,*

²*TLK Energy GmbH*

Executive Summary

Developing metallic latent thermal energy storages for replacement of battery capacity might enhance battery electric buses or trains by reduction of storage investment costs, mass, and volume. However, the development of reliable high temperature components requires careful consideration of thermal and mechanical loads, which arise over their service life. In this work, a MATLAB program to investigate the thermal loads on a metallic latent heat storage used in a battery electric bus over its service life was developed. The model was used to study the influence of locations in different climate zones, operation strategy, vehicle type and setup with a heat pump on the occurrence of different state of charge levels of the storage system. The results provide boundary conditions for application related component design and emphasize the wide span of requirements. Thus, the aimed scenario should be considered carefully when designing reliable components for metallic latent thermal energy storages.

Keywords: Heavy Duty electric Vehicles & Buses; Energy storage systems; Packaging, Cooling, & Heat Transfer; Modelling & Simulation; Thermal management

1 Introduction

Battery electric buses (BEBs) and trains have shortcomings compared to diesel vehicles due to high investment costs and limited range, which depend on the ambient conditions, especially when heating is required [1][2]. The investment cost for electric vehicles as well as battery mass and volume can be reduced by replacing part of the battery with a metallic Latent Thermal Energy Storage (mLTES) based on metallic Phase Change Materials (mPCM) [3].

MLTES are operated in a broad temperature range (e.g. room temperature to 650 °C), experience high thermal gradients and thermal cycling, and incorporate temporarily liquid alloys which are highly corrosive to conventional structural materials [4–7]. All of these challenges depend from both the level and duration of temperatures a mLTES experiences over its service life. For example, the temperature dependence of the reaction rate constant k between mPCM and a potential container material can be modelled by the Arrhenius equation:

$$k = A \cdot \exp(-E_a/RT) \quad (1)$$

where T is the absolute temperature, A is the pre-exponential factor, E_a is the molar activation energy and R is the universal gas constant. Thus, an increased temperature enhances the reaction rate and a potential reaction would be progressed more after a certain period of time at this temperature.

The level and duration of temperature experienced over its lifetime depend strongly on the scenario in

which the mLTES is operated and designed for. In this work, a MATLAB program to investigate the influence of the operation scenario on the thermal loads on a mLTES used in a BEB over its service life is presented.

2 Model description

2.1 Model for temperature load analysis

The temperature load analysis was modelled using a custom-built MATLAB program. The storage temperature depends from the state of charge SoC :

$$SoC = Q / C \quad (2)$$

(Q : energy stored, C : net storage capacity). In order to find the occurrence of SoC -levels, at first the storage capacity C was defined for different parameter values, which are:

- Operation profile: In the overnight charging scenario (O), the BEB is fully charged at the bus terminal at night. In the mixed charging scenario (M), overnight charging is combined with opportunity charging at intermediate stops during the daily driven route.
- Vehicle type: A regular 12 m bus and a people mover (5 m bus with capacity for 15 passengers) referred to as 'small bus' were considered.
- Location: Climate data for three locations (Edmonton, Oslo and Berlin) were used from Meteostat [8].
- The studied scenarios were modified regarding whether the vehicle is equipped with a CO₂ heat pump (Model: UltraLight 700EM) by Konvekta [9].

An overview of all studied scenarios is shown in Table 1.

Table 1: Scenarios for quantification of thermal loads.

Scenario	Operation mode	Vehicle Type	Location	Heat Pump	Scenario	Operation mode	Vehicle Type	Location	Heat Pump
1	M	12 m	Edmonton	Yes	13	O	Small	Oslo	Yes
2	M	12 m	Oslo	Yes	14	O	Small	Oslo	No
3	M	12 m	Berlin	Yes	15	M	12 m	Berlin	No
4	M	12 m	Edmonton	No	16	O	12 m	Berlin	Yes
5	M	Small	Edmonton	Yes	17	O	12 m	Berlin	No
6	O	12 m	Edmonton	Yes	18	M	Small	Berlin	Yes
7	O	12 m	Edmonton	No	19	M	Small	Berlin	No
8	M	12 m	Oslo	No	20	O	Small	Berlin	Yes
9	O	12 m	Oslo	Yes	21	O	Small	Berlin	No
10	O	12 m	Oslo	No	22	M	Small	Edmonton	No
11	M	Small	Oslo	Yes	23	O	Small	Edmonton	Yes
12	M	Small	Oslo	No	24	O	Small	Edmonton	No

For each scenario, storage dimensions are calculated in order to cover heating demand on the coldest day of the scenario. The heating demand of the 12 m bus was conducted from a literature review (cf. sections 2.2 and 3.1) and the heating demand of the small bus was investigated via a parametric study based on Modelica modelling (cf. sections 2.3 and 3.1). An intelligent charging strategy is assumed in which the storage is only charged up to a certain SoC to guarantee that $SoC > 0$ is always maintained.

The resulting optimized Q -course of the coldest day is shown in Figure 1 exemplarily for scenario 1. From this curve, the net thermal storage capacity C (maximum value of the curve), the net thermal charging power P_{charge} (maximum positive slope of the curve) and the net thermal discharging power $P_{discharge}$ (maximum negative slope of the curve) are deduced. The results of the dimensioning for all considered scenarios are shown in Figure 2.

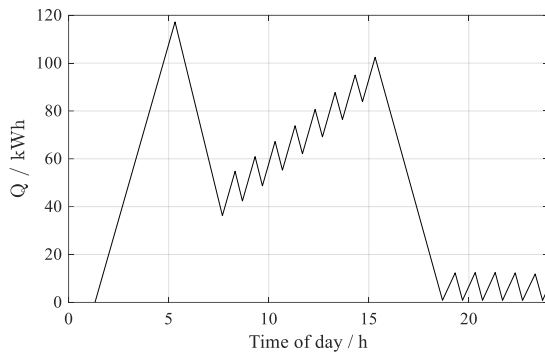


Figure 1: Optimized Q -course for the coldest day of scenario 1.

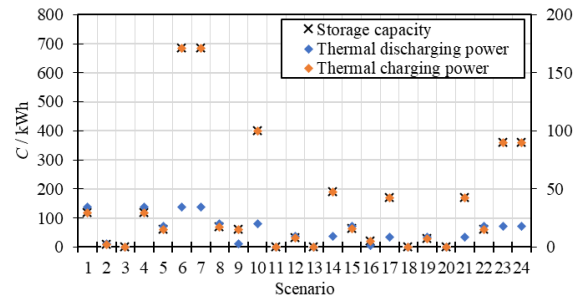


Figure 2: Result of dimensioning of mLTES for different scenarios.

The relation between storage temperature ϑ and SoC depends from the storage configuration and is shown in Figure 3 (a) for scenario 1 and the studied configuration, in which Al-12wt.%Si was considered as mPCM. The lowest defined temperature ($SoC = 0$) of a thermal energy storage system is the temperature down to which thermal energy can be provided at nominal power. It depends on the effectiveness of the heat extraction system and can range from, for example, 100 °C to 350 °C for different systems. In this study, the lowest defined temperature was assumed to be 200 °C.

Now, hourly ambient temperature data of the selected location in a five-year period is considered. The optimized Q -course is determined for every day similar to the approach described for the dimensioning at the coldest day. By using the previously defined $\vartheta(Q)$ -function, a daily temperature course of the storage can be found. Therefore, a linearly spaced temperature array with 10 K steps is defined. For each day, it is checked in five-minute intervals within which temperature level the storage is situated and a five-minute duration value is added to a duration array in the related temperature line. Afterwards, all daily duration arrays for the five years are summed up and divided by five in order to get the yearly duration array. If the storage is at a certain temperature level it means, that it is below the upper temperature limit of the temperature interval. The first entry of the array includes all durations in which the storage is below the lowest defined temperature, such as when $SoC = 0$. In this entry, it is not defined whether the storage has a temperature of e.g. 20 °C, 100 °C or 200 °C. The lowest defined temperature of a thermal energy storage system is the temperature, up to which thermal energy can be provided with nominal power. It depends from the effectiveness of the heat extraction system and can be in the range of e.g. 100 °C to 350 °C for different systems. In this study, the lowest defined temperature was assumed to be 200 °C.

The result of this stage is a histogram, which is exemplarily shown for scenario 1, which is representative for scenarios with less time at raised temperatures, and scenario 4, which is representative for scenarios with a broad temperature duration distribution in Figure 3 (b) and (c).

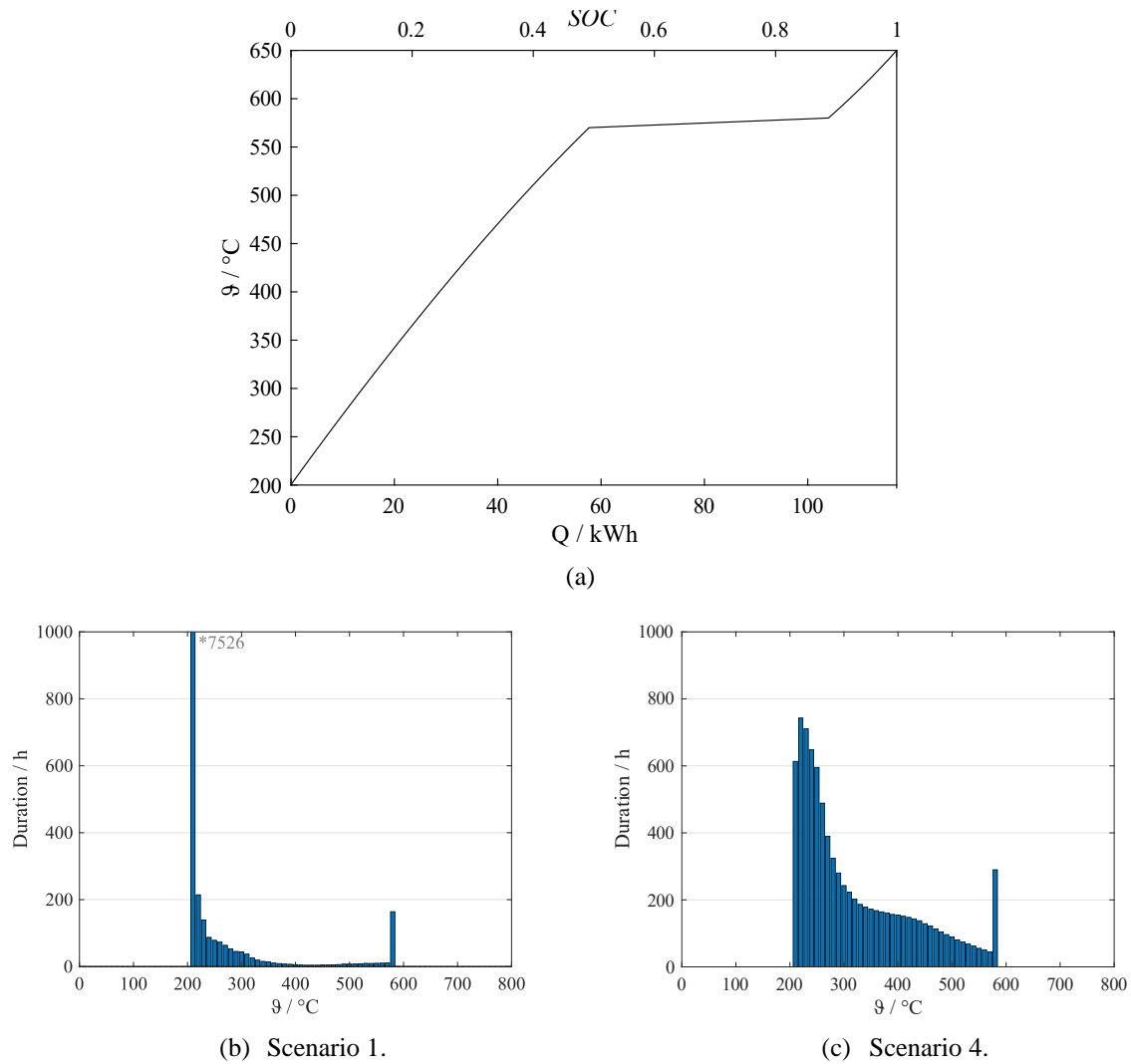


Figure 3: (a) Relation between storage temperature θ and net amount of energy in the storage Q and the net SoC respectively, exemplarily shown for scenario 1. (b) – (c): Storage temperature histograms per year exemplarily shown for two scenarios.

2.2 Model for heating demand of a 12 m bus

Since a 12 m bus is a quite common vehicle, the heating demand is also well described in literature. Due to this, a literature study was conducted to determine the temperature dependent heating demand. In total, three different studies were considered for this work as reference. Basile et al. [10] measured the heating demand of a 12 m bus heated with a fuel-powered heater in dependence of the ambient temperature. Dicke [11] conducted a linear model based on data determined experimentally by Knote et al. [12], who carried out measurements at two BEBs. Vehviläinen et al. [14] collected data from four BEBs and one hybrid bus in Tampere (Finland) for three years between January 2017 and August 2021. The values given are the electric energy consumption by the electric resistance heating system per kilometer in kWh/km. For comparing the heating demand in W, we assumed an average bus speed of 15 km/h, which is a reasonable estimation for the bus route considered in the study.

Out of the three different literature references, an average value for each temperature was calculated. For transferring the average value into the simulation model, the average value was fit into a linear model.

2.3 Model for heating demand of a small bus

The heating demand of a small bus was investigated by a computational method. As part of the method, the effects of various physical influences on the heating demand were investigated and quantified.

In order to identify the main influencing factors, a simulation-based full fractional parameter study with a Modelica lumped-parameter-model of the bus cabin was performed using the total parameter range.

Afterwards, a limited parameter study using a subset of the total parameter range was performed in order to investigate steady state heating demand. The parameter ranges used, both in the full fractionally study as well as in the limited parameter study, are listed in Table 2. The air exchange was calculated in accordance with VDV-Schrift 263 11/2018 and VDI 2078. The solar irradiation and ambient temperature for the limited parameter study are related to Test-Reference-Year (TRY) 2010 for weather zone 6 (Aachen area) in hourly resolution by DWD. Bus orientation towards sun and shading was considered.

The method was then applied to a people mover with 4.9 m in length and a capacity of 15 passengers for a plausible worst-case scenario in terms of heating. The heating demand is maximum for no passenger occupation, maximum air exchange, low ambient temperature and low solar irradiation. However, a high air exchange (through door opening) without passengers is not reasonable, which is the reason why a passenger occupation of 50% was assumed for the worst-case scenario. Furthermore it was assumed, that the bus is mainly operated during day-time. Thus, data outside the period from 6 a.m. to 8 p.m. are excluded from the analysis.

Table 2: Parameter ranges used in full fractional and limited parameter study.

Parameter	Range in full fractional study	Value or range in limited parameter study
Window-Area Side Walls	20 – 80%	50 %
Thermal Transmittance Walls	0.5 – 3.5 W/(m ² K)	2.57 W/(m ² K)
Thermal Transmittance Windows	0.5 – 6 W/(m ² K)	15 W/(m ² K)
Solar Transmittance Windows	30 – 90%	45%
Air Exchange Rate	0 – 75 V _{cabin} /h	10 – 40 V _{cabin} /h
Passenger Occupation	0 – 100%	0 – 100%
Solar irradiation	Solar irradiation: 0 – 500 W/m ²	Weather data (Aachen, TRY 2010)
Ambient temperature	-15 – 35 °C	Weather data (Aachen, TRY 2010)

3 Results and discussion

3.1 Heating demand

The linear model for the heating demand \dot{Q}_{12m} of a 12 m bus depending on the ambient temperature ϑ_{amb} , resulting from a literature review, is given in equation (3).

$$\dot{Q}_{12m} = (11920 - 574 \cdot \vartheta_{amb} / ^\circ\text{C}) \text{ W} \quad (3)$$

The heating demands in dependence of the ambient temperature for all literature references, the average value and the linear model of the average value, are shown in Figure 4.

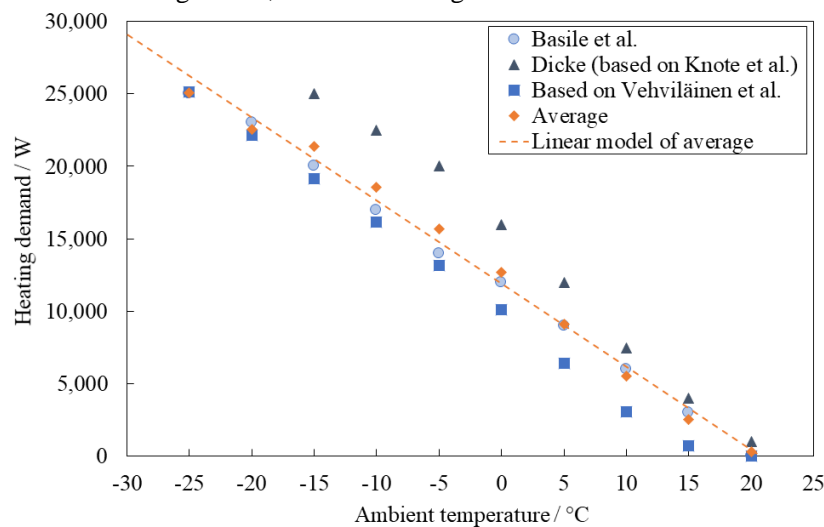


Figure 4: Heating demand \dot{Q}_{12m} of a 12 m bus in dependence of the ambient temperature ϑ_{amb} .

Regarding the computational method for heating demand investigation of small busses, the full fractional study revealed the parameters influencing heating demand the most. The main influencing factor is the ambient temperature, followed by air exchange rate and solar irradiation. The other factors investigated show a comparatively low influence on heating demand.

Heating and cooling demands for the worst-case heating scenario are shown in Figure 5 in dependence of ambient temperature intervals. Cooling demands are also depicted that were investigated as part of another study and are not discussed in detail in this article. The maximum heating power was found to be 10 kW at -9 °C, when no solar irradiation hits the vehicle cabin. This was the lowest ambient temperature at the investigated location Aachen in test reference year 2010 within the studied range of day-time. It is recommended to use this determined maximum heating power for dimensioning the thermal energy storage system.

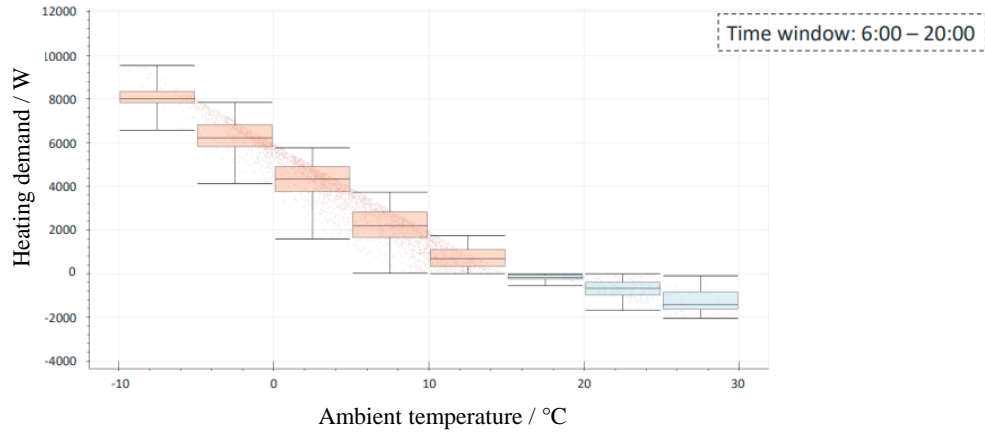


Figure 5: Heating demand \dot{Q}_{small} of a small bus in dependence of the ambient temperature ϑ_{amb} for the heating worst-case, operated during day-time in Aachen for the test reference year 2010.

In order to use the heating demand of a small bus as input for the yearly temperature load analysis of a thermal energy storage, a linear model for the heating demand was derived from the average values of the heating cases shown in Figure 5. The resulting linear model is given in equation (4).

$$\dot{Q}_{small} = (4543 - 337 \cdot \vartheta_{amb} / ^\circ\text{C}) \text{ W} \quad (4)$$

3.2 Temperature load analysis

The resulting storage temperature histograms are compared by presentation as box-whisker-plots. Additionally, the yearly duration in liquid state d_{liquid} is evaluated. It is the sum of durations in which the storage temperature is higher than the mPCM melting temperature (577 °C for Al-12wt.%Si). The box-whisker-plots for yearly duration at certain ϑ -intervals for all scenarios are shown in Figure 6.

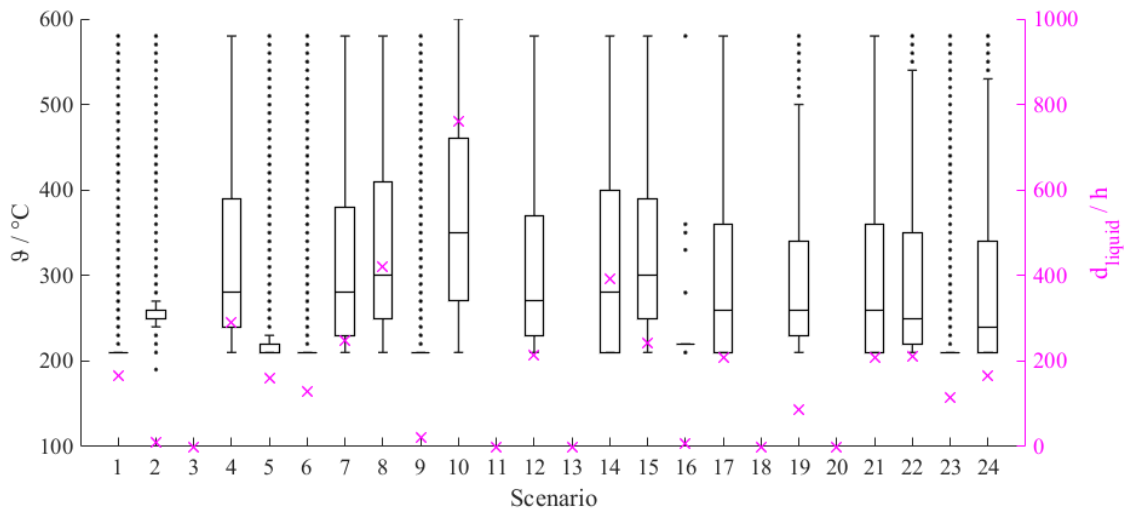


Figure 6: Box-whisker-plots for yearly duration at certain storage temperature intervals and yearly duration in liquid state for all scenarios.

In the scenarios in Berlin with a heat pump equipped and in small buses with a heat pump in Oslo, no mLTES is required at all, as the heat demand can be provided by the heat pump alone. The overnight charging scenarios result in very high storage capacities of 170 – 685 kWh. In regions where a heat pump would not work on the coldest day (e.g. Edmonton), a heat pump installation does not affect the storage dimension.

The scenario with the highest temperature load (highest median temperature, highest quantile, highest duration in liquid state with 761 h/year) is scenario 10: A 12 m bus in Oslo with overnight charging strategy and without heat pump. Due to the thermal storage being the only heating system, it is active at moderate ambient temperatures already. Furthermore, the yearly ambient temperature distribution is narrower than in Edmonton, thus the storage is not as oversized for certain cases as it is in Edmonton, where extreme minimum ambient temperatures occur. The scenario with the lowest temperature load (lowest median temperature, lowest quantile, lowest duration in liquid state (which is $\neq 0$) with 6 h/year, lowest amount of outliers) is scenario 16: A 12 m bus in Berlin with mixed charging strategy and with heat pump. This is because most but not all of the heating cases in Berlin can be covered with the heat pump alone in this scenario.

This study considers average storage temperatures only and does not consider local differences in temperature inside the storage. In reality it is expected, that during charging the storage material would start melting at the location of the charging components and thus this interface might experience a longer duration of liquid metal contact than other locations within the storage. Similarly it is expected, that during discharging, storage material solidification would start at the location of heat exchanger components which would lead to a shorter duration of liquid metal contact. The evaluation of d_{liquid} gives a maximum duration for which any location in the storage would be in liquid metal contact.

4 Conclusion

This study provides detailed time-temperature curves which can serve as boundary conditions for application related reaction analysis. The wide span of 6 to 761 h/year in liquid state shows, that depending from the scenario, very different requirements arise to reliable storage components. For some scenarios, container components with a certain reactivity in contact with liquid mPCM could be operated over the service life, but would not suit for other scenarios. Thus, the aimed scenario always needs to be considered when designing reliable components and especially container solutions for mLTES. In a next step, the influence of storage configuration (storage material, material class weight fractions and operation temperature range) on the thermal loads over service life could be investigated.

Acknowledgments

This research was partially funded by EFRE (Europaischer Fonds für regionale Entwicklung) Leitmarktwettbewerb NRW (Nordrhein-Westfalen) Mobilität.Logistik within the project ‘Lathe.Go’, grant number EFRE0801688 and by the Ministry of Economic Affairs, Labour and Tourism Baden-Württemberg within the project ‘MELABUS’, grant number BW7-2122/02.

References

- [1] W. Kraft, V. Stahl, P. Vetter, Thermal Storage Using Metallic Phase Change Materials for Bus Heating—State of the Art of Electric Buses and Requirements for the Storage System, *Energies* 13 (2020) 3023. <https://doi.org/10.3390/en13113023>.
- [2] S. Yang, S. von Mach, J. Buschbeck, S. Donner, W. Kraft, Thermische Hochleistungsspeicher für batterieelektrische Schienenfahrzeuge, *ZEVRail* 2022 (2022) 43–49.
- [3] W. Kraft, A. Rawson, V. Stahl, P. Vetter, F. Kargl, M. Sonnekalb, P. Best, Thermal high-performance storages as heating systems for electric buses, in: *Proceedings of 8th Transport Research Arena TRA 2020*, 2020.
- [4] A.J. Rawson, W. Kraft, T. Gläsel, F. Kargl, Selection of compatible metallic phase change materials and containers for thermal storage applications, *Journal of Energy Storage* 32 (2020) 101927. <https://doi.org/10.1016/j.est.2020.101927>.
- [5] R. Fukahori, T. Nomura, C. Zhu, N. Sheng, N. Okinaka, T. Akiyama, Thermal analysis of Al–Si alloys as high-temperature phase-change material and their corrosion properties with ceramic materials, *Applied Energy* 163 (2016) 1–8. <https://doi.org/10.1016/j.apenergy.2015.10.164>.
- [6] A. Dindi, N. Lopez Ferber, D. Gloss, E. Rilby, N. Calvet, Compatibility of an Aluminium-Silicon metal alloy-based phase change material with coated stainless-steel containers, *Journal of Energy Storage* 32 (2020) 1–18. <https://doi.org/10.1016/j.est.2020.101961>.
- [7] V. Tiwari, S. Periaswamy, Compatibility of structural materials with AlSi12 alloys-based phase change material and increasing the corrosion resistance by ceramic coatings, *Journal of Energy*

- Storage 2023 (2023) 1–8. <https://doi.org/10.1016/j.est.2023.108526>.
- [8] Meteostat, The Weather's Record Keeper. <https://meteostat.net/en/> (accessed 19 June 2024).
- [9] Konvekta AG, Datenblatt Ultra Light 700EM CO2 HP, Schwalmstadt, 2020.
- [10] Robert Basile, Helmut Scheid, Dietmar Tanke, Markus Moeseler, Ralf Häring, Beheizungsstrategien für Elektrobusse, 2017.
- [11] Niklas Dicke, Untersuchung und Optimierung von Konzepten thermischer Hochleistungsspeicher. Masterarbeit, Stuttgart, 2019.
- [12] T. Knotte, B. Haufe, L. Saroch, E-Bus-Standard: Ansätze zur Standardisierung und Zielkosten für Elektrobusse. Förderkennzeichen 16EM3103-1 (2017).
- [13] H. Basma, C. Mansour, M. Haddad, M. Nemer, P. Stabat, Comprehensive energy modeling methodology for battery electric buses, Energy 207 (2020) 118241. <https://doi.org/10.1016/j.energy.2020.118241>.
- [14] M. Vehviläinen, R. Lavikka, S. Rantala, M. Paakkinen, J. Laurila, T. Vainio, Setting Up and Operating Electric City Buses in Harsh Winter Conditions, Applied Sciences 12 (2022) 2762. <https://doi.org/10.3390/app12062762>.

Presenter Biography



Veronika Stahl obtained her Master's degree in material science at University of Stuttgart and is currently a doctoral candidate in the field of automotive engineering. Since 2018, Veronika is researcher at the Institute of Vehicle Concepts of German Aerospace Center. She is part of a team investigating metallic latent thermal energy storage systems for the application in battery electric vehicles like buses or trains. Her academic work focuses the development of reliable containments for metallic phase change materials which suit as storage material in the considered system.